Materials Advances

ROYAL SOCIETY OF CHEMISTRY

PAPER

View Article Online
View Journal | View Issue

Cite this: *Mater. Adv.*, 2025, **6**, 5588

Dual-functional tannic acid-infused AgNPs-PVDF membranes *via* coagulation methods: an integrated study on antibacterial and antifouling performances for oil-in-water separation

Irshad Kammakakam, *[a] Ishfaq Showket Mir,[bc] Nadeem Baig, *[d] Ali Riaz[c] and Younés Messaddeq[c]

Recently, the development of dual-functional surfaces combining antibacterial and antifouling properties has remarkably gained significant attention in membrane separation technologies, particularly for oil-in-water separations. Herein, we present a novel approach to synthesizing PVDF mixed matrix membranes using the phase inversion process, with different concentrations of tannic acid and silver nitrate *via* the coagulation bath method of fabrication, a naturally inspired tannic acid (TA)-based green chemistry strategy to facilitate the simultaneous benefit of combining high antifouling ability as well as antibacterial activities. A controlled approach for the *in situ* incorporation of AgNPs into the mixed-matrix membrane was successfully achieved using an active coagulation bath. We have specifically focused on the various concentrations of TA in the membranes to serve as a multifunctional component *via* an exclusive coagulation method of fabrication, which further enables integration and dispersion of AgNPs into the PVDF matrix. As such, five different membranes (M-1 to M-5) with distinct amounts of TAs were prepared and investigated for their structural properties, primarily antibacterial activities and separation performances, including pure water flux in cross-flow filtration and rejection of an oil-in-water emulsion. The M-2 and M-3 membranes, containing moderate amounts of tannic acid, demonstrated superior rejection and flux recovery with more than 90% oil-in-water emulsion. These membranes also exhibited optimized performance in antifouling resistance when tested with synthetic natural organic matter (NOM) solutions. Most interestingly, all the membranes showed extraordinary antibacterial properties against *E. coli* when tested with the disk diffusion method. Overall, the unique surface chemistry obtained by synergistic effects of the TA-AgNPs combination resulted in enhanced performance of these membranes toward superior antibacterial and desirable antifouling properties, yielding new PVDF matrix candidates for advanced oily wastewater treatments.

Received 12th April 2025,
Accepted 20th June 2025

DOI: 10.1039/d5ma00355e

rsc.li/materials-advances

1. Introduction

Membrane technology has emerged as a cornerstone in water treatment and purification processes, offering a versatile and efficient approach to address global water scarcity and contamination challenges.[1–4] The ability of membranes to selectively separate contaminants from water at the molecular level has revolutionized various industries, from desalination to wastewater treatment. Among the diverse array of membrane materials available, polyvinylidene fluoride (PVDF) has gained significant attention due to its exceptional chemical resistance, thermal stability, and mechanical strength.[5–8] These properties make PVDF membranes particularly suitable for applications in harsh environments and for treating complex water streams.[9] However, despite their numerous advantages, PVDF membranes are not without limitations, primarily stemming from their inherent hydrophobic nature.[10]

The hydrophobicity of PVDF membranes presents several challenges that hinder their widespread adoption and long-term efficiency in water treatment applications.[11] Foremost among these is the issue of membrane fouling, a phenomenon where contaminants adhere to the membrane surface or become entrapped within its pores, leading to a significant

[a] *Department of Chemistry, Nazarbayev University, 53 Kabanbay Batyr Ave, 010000, Astana, Kazakhstan. E-mail: irshad.kammakakam@nu.edu.kz*
[b] *Département de Chimie, Faculté des Sciences et de Génie, Université Laval, Québec, QC, G1V 0A6, Canada*
[c] *Centre d'optique, Photonique et laser, 2375 Rue de la Terrasse, Université Laval, Québec, QC, G1V 0A6, Canada*
[d] *Interdisciplinary Research Centre for Membranes and Water Security, King Fahd University of Petroleum and Minerals, Dhahran, Saudi Arabia. E-mail: nadeembaig@kfupm.edu.sa*

decline in permeate flux and separation efficiency over time.[12–14] This fouling problem is particularly pronounced when dealing with oily waters or solutions rich in organic matter, as these substances have a strong affinity for hydrophobic surfaces. Additionally, the hydrophobic character of PVDF membranes results in lower water permeation rates compared to their hydrophilic counterparts, necessitating higher operating pressures and consequently increased energy consumption.[15,16] These limitations not only reduce the overall performance of PVDF membranes but also escalate operational costs and maintenance requirements in water treatment facilities.

To address these challenges, researchers have explored various strategies to enhance the performance of PVDF membranes. Surface modification techniques, such as plasma treatment, grafting, and coating, have been extensively investigated to impart hydrophilicity to the membrane surface, thereby improving its antifouling properties and water permeability.[17–23] Another promising approach involves the incorporation of nanoparticles, such as TiO_2, ZnO, and Ag, into the membrane matrix or surface to confer additional functionalities like photocatalytic activity, antimicrobial properties, and enhanced mechanical strength.[24–27] Several studies have reported the grafting of zwitterionic polymers onto PVDF membranes, which significantly improved their resistance to organic fouling.[28,29] However, the long-term stability of these grafted layers in harsh chemical environments remains a concern.[30] Similarly, some studies have investigated the incorporation of graphene oxide nanosheets into PVDF membranes, which enhanced their antifouling properties against oil emulsions.[31,32] While effective, the potential for nanoparticle leaching and its environmental impact requires further investigation.

Another strategy that has gained attention is the development of composite membranes.[33–35] A recent study fabricated a PVDF/TiO_2 composite membrane with photocatalytic properties, demonstrating improved flux recovery and organic matter degradation under UV irradiation.[25] However, the application of this technology is limited by the need for an external light source and the potential formation of harmful byproducts during the photocatalytic process. Membrane surface patterning has also been explored as a means to reduce fouling.[36,37] A study investigated micro-patterned PVDF membranes that exhibited enhanced antifouling performance due to improved hydrodynamics at the membrane surface.[38,39] Despite these promising results, the scalability of such precise surface patterning techniques for large-scale membrane production remains a significant challenge.

On the other hand, contaminants in oily wastewater contain not only complex organic matter but also various bacteria, which are detrimental to the membranes as they form biofilms and cover the surfaces of the membrane partially or even completely, leading to a significant depletion of flux.[40,41] Therefore, the fabrication of a high-performance membrane matrix ideally requires an offering of both extraordinary antifouling and antibacterial performance in oil/water emulsion separations. There have been various studies introducing metallic or non-metallic nanomaterials to disrupt bacterial growth and inhibit the formation of biofilms on the surface of wastewater treatment membranes.[42–45] Among them, silver nanoparticles (AgNPs) have attracted great attention to mitigate the growth of bacteria with strong anti-bacterial activity, mainly used for biomedical applications. Nevertheless, oily wastewater treatment demands relatively green chemistry pathways in separation and purification technology. Keeping this in mind, utilizing a nature-inspired biomacromolecule such as tannic acid (TA) acting as both an anti-bacterial and a potential reducing agent for the synthesis of silver nanoparticles could be a better option.[46] Furthermore, it is already evident that tannic acid contributes to the enhancement of hydrophilicity of polymeric membrane matrices, making dual functional TA/Ag nanoparticle-based fillers for enhanced oil-in-water separation applications while simultaneously providing anti-bacterial and antifouling performances (Fig. 1).

Given the above-mentioned persistent challenges, this study exclusively investigates the development of a new approach to combine the distinct benefits of tannic acid and Ag NPs *via* a coagulation bath fabrication method, yielding novel TA/Ag NP-induced PVDF mixed matrix membranes, anticipating enhancement in antifouling and antibacterial properties while offering high performances toward oil-in-water emulsion separations.

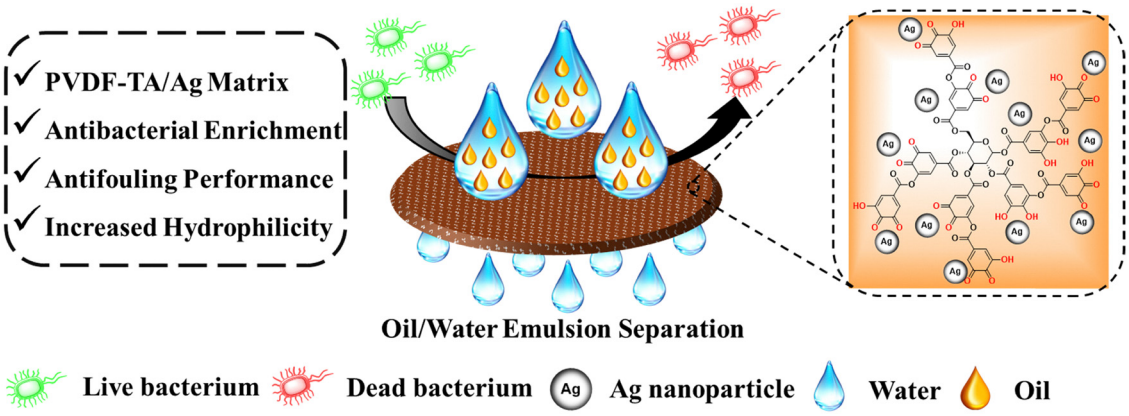

Fig. 1 Schematic representation of the newly developed tannic acid-infused silver nanoparticle-decorated PVDF membrane explicating superior antibacterial activities and enhanced oil-in-water separation.

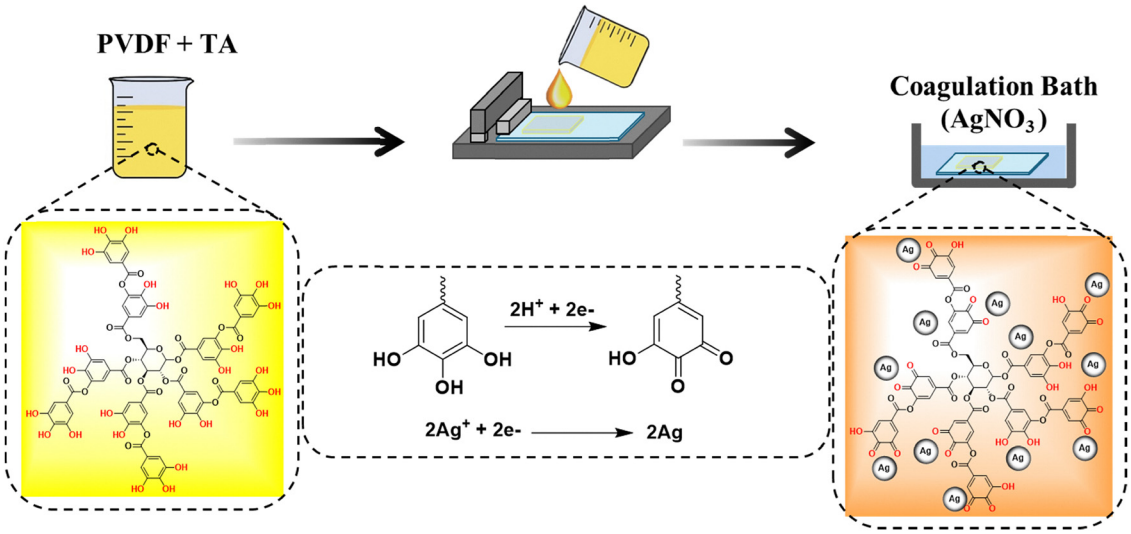

Scheme 1 Schematic illustration of TA-infused AgNPs PVDF membrane fabrication *via* the green approach of the coagulation method for oil-in-water separation.

As such, by utilizing the phase inversion process of TA-impregnated PVDF with silver nitrate ($AgNO_3$) in the coagulation bath, a unique and tailored surface chemistry is developed that effectively resists foulant adhesion while simultaneously exhibiting antimicrobial activity. On the other hand, according to our previous investigations, we have also introduced the benefits of polyvinylpyrrolidone (PVP) as a pore-forming agent in the TA/PVDF matrix, foreseeing the enhancement of the membrane's performance by optimizing its pore structure and distribution. Overall, central to our approach is the multifunctional role of TA, which not only contributes to the membrane's antifouling properties but also facilitates the integration and dispersion of silver nanoparticles within the PVDF matrix while enhancing hydrophilicity, as depicted in Scheme 1. This synergistic combination of TA and AgNPs is expected to address the dual challenges of organic fouling and microbial contamination, which are particularly challenging in the treatment of oily waters and effluents rich in natural organic matter. This study aims to contribute to the ongoing efforts in membrane technology by offering a potentially scalable and effective solution to enhance the efficiency, longevity, and applicability of PVDF membranes in challenging water treatment scenarios.

2. Materials and methods

2.1. Materials

PVDF-44080 was obtained from Alfa Aesar. $AgNO_3$, polyvinylpyrrolidone (PVP) Mw ~ 40 000 and *N*,*N*′-dimethylacetamide were purchased from Sigma Aldrich. All other chemicals were obtained from commercial sources and used as received.

2.2. Synthesis of mixed matrix membranes

Various PVDF membranes were synthesized using the phase inversion process. Before the various PVDF dope solutions were prepared, the PVDF powder was dried overnight at 60 °C. Then, 15% of the PVDF dope solution was prepared by adding the PVDF powder to dimethylacetamide. 2% PVP was added to all dope solutions as the pore-forming agent. In preparing the M-2, M-3, M-4, and M-5 membranes along with PVDF and PVP, TA was added at 0.2, 0.4, 0.6, and 1%, respectively. All dope solutions were prepared in an oil bath by heating at 60 °C for 12 hours under continuous stirring. A thin film of the dope solutions was prepared with the help of a membrane applicator on a glass plate and immediately dipped into the coagulation bath for the phase inversion process. For the M-1 membrane, the coagulation bath consisted of double distilled water, whereas for the synthesis of the M-2, M-3, M-4, and M-5 membranes, the coagulation bath consisted of 0.0025 M $AgNO_3$ (Table 1).

2.3. Characterizations

The morphology and microstructure of the membranes were examined using scanning electron microscopy (SEM). Before imaging, the specimens were mounted on holder stubs and vacuum-dried for 24 hours. They were then sputter-coated with gold to ensure conductivity, and SEM images were captured at an accelerating voltage of 15–20 kV. Imaging was performed using a Quanta™ 250 field-emission environmental scanning electron microscope equipped with a Schottky field emission gun, operating at 10 kV.

FTIR spectra of all membrane samples were recorded on an Invenio-R FTIR Spectrometer (Bruker Ltd, Canada) equipped

Table 1 Composition of the various PVDF membranes

Membranes	PVDF (%)	Tannic acid (%)	DMA (%)	PVP (%)	Coagulation bath ($AgNO_3$)
M-1	15	0	83	2	0
M-2	15	0.2	82.8	2	0.0025 M
M-3	15	0.4	82.6	2	0.0025 M
M-4	15	0.6	82.4	2	0.0025 M
M-5	15	1	82	2	0.0025 M

with a nitrogen-cooled MCT detector. The spectra were averaged over 64 scans acquired in the wavenumber range of 500–4000 cm^{-1} at a spectral resolution of 4 cm^{-1}. The experimental setup and data recording were managed using OPUS software (Bruker, USA).

To examine the surface wettability of these membranes, contact angle measurements were performed at 24 °C in a video-based contact angle system model FTA200 (First Ten Angstroms, Inc.) using the sessile drop method. A water droplet of 0.5 μL was placed on the membrane using a syringe with a needle diameter of 0.525 mm. Contact angle measurements were recorded from the software (FTA 32) by analyzing the shape of the distilled water drop after it was placed over the membranes.

The surface charge of the membranes was evaluated by measuring the zeta potential using a SurPASS Electrokinetic Analyzer. The streaming potential was generated by applying a controlled pressure increase up to 250 mbar across a channel, which was formed by stacking the membranes between layers of PTFE film. The background solution used was 10 mM KCl, with an initial pH of 2. To adjust the pH, precise amounts of 0.1 M HCl and 0.1 M KOH were automatically added to the test solution. For each pH value, three washing cycles and four zeta potential measurements were conducted to ensure accuracy.

2.4. Antibacterial tests

The test started with defrosting the 1 mL Eppendorf tube containing bacterial strains of model Gram negative *E. coli* (from the stock stored at −80 °C) by carefully submerging in lukewarm water for 5 minutes to defrost the contents. At the same time, TSB (tryptic soy broth) was prepared at 30 g L^{-1} and autoclaved for 15 minutes at 121 °C. After autoclaving, TSB was allowed to cool down and 10 mL of it was poured into each of 4 test tubes. The bacterial strains were inoculated in test tubes containing 10.0 mL of sterile TSB and then cultured in a shaking incubator (37 °C, 230 rpm) for 6 h. In another test tube containing 10.0 mL sterile TSB, 200 μL bacterial solution was subcultured to make the turbidity equal to 0.5 McFarland ($\sim 1.5 \times 10^8$ CFU mL^{-1}). The bacterial cultures were collected after 6 h and were subjected to centrifugation (4500 rpm, 5 min), with the resultant residue rinsed multiple times with phosphate-buffered saline (PBS) to yield bacterial pellets. The membrane samples were pre-drilled with a 5 mm sterile hole puncher. The obtained round membranes were subjected to UV-sterilization on both sides for 15 minutes.

The M-1, M-2, M-3, M-4 and M-5 membranes were tested for antibacterial activity against *E. coli* by the disk diffusion method. Agar slants were prepared with a concentration of 15 g L^{-1} in 30 g L^{-1} of LB media spread with 100 μL *E. coli* culture and incubated overnight at 37 °C. Post-incubation, the inhibition zone, which is the area between the radius of the pellicles, and the distance of the bacterial colonies to the pellicle centers were observed and measured by averaging results from three independent experiments.

2.5. Membrane pure water flux

The pure water flux of the membranes was evaluated using a crossflow filtration unit equipped with a cross-flow assembly, which held membranes with an active surface area of 21 cm^2. Prior to flux measurements, the membranes were primed at 2 bar for 30 minutes to stabilize their performance. The pure water flux was then measured across a range of pressures, from 0.5 bar to 2.5 bar, to assess their behavior under varying pressure conditions. The permeate was collected and pure water flux (J, L m^{-2} h^{-1} as unit, abbreviated as LMH) of the membranes was calculated using eqn (1)

$$J_w = \frac{V}{A \times t} \quad (1)$$

where V is the volume of permeate collected (L), A is the effective filtration area (m^2) and t is the time of filtration (h).

2.6. Oil in water emulsion

Surfactant-stabilized oil-in-water (O/W) emulsions were prepared using the previously described method with slight modifications.[47] In summary, 0.2 g of diesel was added to 1 L of water and stabilized with 0.5 g of SDS. To achieve a stabilized emulsion, the mixture was vigorously stirred for 24 hours until a milky-colored emulsion was obtained.

The anti-fouling performance of the membranes was assessed by filtering a diesel-in-water emulsion using a cross-flow filtration setup. The evaluation consisted of three filtration and washing cycles, each lasting 1 hour. Initially, the oil-in-water emulsion was filtered, and the flux decline was recorded over the course of 1 hour for each membrane. Following this, the membranes were flushed and washed with deionized water, after which the flux recovery was measured by running pure water through the system for 1 hour. These fouling and washing cycles were repeated, continuing for a total duration of 6 hours. To determine the anti-fouling aspects of these membranes, two methods were adopted for membrane cleaning. In the first method, DI water was used to clean the membranes by cross-flow shear velocity. The PWF of the membranes was recorded after cleaning with DI water. In the second method, the same procedure was adopted, except that instead of DI water, a 0.05 M NaOH solution was used as the cleaning solution. The reusability of the membranes was evaluated by calculating the flux recovery ratio (FRR) of the membranes using the pure water flux.

$$\mathrm{FRR}\ (\%) = \left(\frac{J_{w_n}}{J_{w_{n-1}}}\right) \times 100\% \quad (2)$$

where J_{w_n} and $J_{w_{n-1}}$ are the water flux in the nth cycle and $(n-1)$th cycle (LMH), respectively.

The separation efficiency of the membranes for oil in water emulsions was measured by a TOC analyzer using a non-dispersive infra-red detector (NDIR) with a supply gas pressure of 254.0 kPa, and carrier gas flow rate of 150 mL min^{-1}. The furnace temperature was maintained at 681 °C and the NDIR temperature set at 65.4 °C. The rejection of the oil in water emulsion was calculated with the equation:

$$R = 1 - \left(\frac{C_p}{C_f}\right) \times 100\% \quad (3)$$

where C_p and C_f are the TOC concentrations in the permeate and feed solutions, respectively.

The membrane's performance stability was continuously evaluated for 9 hours while separating a 200-ppm oil-in-water emulsion. The rejection was monitored every hour using eqn (3).

2.7. Organic fouling tests

Organic fouling tests were performed on the best-performing membranes from oil-in-water emulsion tests (M-1, M-2, M-3) using a synthetic natural organic matter (NOM) solution. The synthetic NOM solution was prepared according to established procedures in the literature. In brief, solutions were made with 50.0 mg of BSA, SA, and HA dissolved separately in 10.0 mM phosphate buffer (pH 7.00), ultrapure water, and 0.10 M NaOH, respectively. The pH of the HA solution was adjusted to 7.00 using 0.50 M and 5.00 M HCl to control the ionization of ionogenic groups. Subsequently, the NOM mixture was prepared by combining 50.0 mg L^{-1} of the BSA, SA, and HA solutions with a solution of 1.00 mM $CaCl_2$ and 7.00 mM NaCl in ultrapure water in a 1 : 1 ratio. The fouling experiments were conducted in the same cross-flow filtration set-up, where the retentate was circulated back to the feed solution under continuous stirring in order to minimize the variation in concentration of feed to the membranes. The NOM solution was run for three cycles of filtration each lasting for 1 h. The membranes were cleaned in between the filtration cycles. To determine the anti-fouling aspects of these membranes, DI water was used to clean the membranes by crossflow shear velocity. The PWF of the membranes was recorded after cleaning with DI water. Flux recovery ratio was calculated using eqn (2).

The NOM content in the feed and permeate solutions was determined by TOC analyzer using a non-dispersive infra-red detector (NDIR) with a supply gas pressure of 254.0 kPa, and carrier gas flow rate of 150 mL min^{-1}. The furnace temperature was maintained at 681 °C and NDIR temperature set at 65.4 °C. The rejection of NOM was calculated with eqn (3).

3. Results and discussion

The initial discussion centers on the synthesis methods of mixed matrix membranes, followed by their functionalization with tannic acid and AgNPs. Subsequent sections delve deeper into the membrane morphology, physicochemical, and antibacterial properties of the membranes, concluding with an analysis of their permeation properties, fouling behavior, and effectiveness in rejecting organic foulants.

3.1. Fabrication and surface morphology characterization of TA-infused AgNP-decorated PVDF membranes.

As outlined in Scheme 1, TA/AgNP composites on a polyvinylidene fluoride (PVDF) matrix membrane were fabricated using a reduction process involving tannic acid and silver nitrate ($AgNO_3$) solution *via* a coagulation method. In this study, we have exclusively aimed to utilize the multifunctional benefits of TA, a nature-inspired biomacromolecule serving both antibacterial activities and superhydrophilic behaviors, which are directly related to the separation efficiency. It is already evident that the tannic acid molecule consists of polygalloyl ester chains, a central core of glucose having multiple ester bonds exhibiting reduction ability, acting as an ideal reducing as well as stabilizing agent. Unambiguously, the reaction mechanism for the formation of AgNPs involves a redox reaction in which TA forms quinones, disrupting the Ag^+/TA complex (Scheme 1).[27,48] This leads to the reduction of Ag^+ ions into Ag atoms, which then aggregate into clusters, eventually yielding AgNPs through further cluster growth upon the conversion of hydroxyl groups of tannic acid into carbonyl groups, enhancing surface absorption interactions of AgNP π electrons present in the multiple carbonyl groups.[49]

Nevertheless, the whole membrane-modification process was carried out with green and low-cost reagents under mild and facile conditions. Considering TA impregnation as a critical step that determined the subsequent formation of the AgNPs, the variation in the concentration of TA was controlled in the dope solution. As such, 15% of the PVDF dope solutions in DMAc having various weight percentages of TA (0, 0.2, 0.4, 0.6, and 1%) were prepared at 60 °C for 12 hours under continuous stirring, and a phase inversion process-led fabrication was then carried out in a coagulation bath consisting of 0.0025 M $AgNO_3$ to obtain new TA/AgNPs PVDF membranes. Hereafter, for convenience's sake, according to the amount of TA, each TA/AgNP PVDF membrane was named M-1, M-2, M-3, M-4, and M-5, respectively. At the same time, it is noteworthy that for the M-1 membrane, the coagulation bath was composed of simple double distilled water to yield pristine PVDF matrix membrane to compare the separation and antibacterial performances of the newly designed TA/AgNPs PVDF matrix membranes.

The surface morphology, cross sections, and microstructure of the newly developed TA/AgNPs-PVDF membranes were further analysed using scanning electron microscopy (SEM), as shown in Fig. 2. The membranes exhibited the characteristic structure of a polymer film formed *via* the phase inversion process.[50–52] The incorporation of AgNPs into the modified membranes was confirmed through energy-dispersive X-ray spectroscopy (EDX) and elemental mapping (M2–M5). Notably, the weight percentage of AgNPs increased from 0.16% to 2.46% from M2 to M5, indicating a direct correlation between tannic acid (TA) concentration in the dope solution and the AgNP loading within the membrane matrix. Since the Ag^+ concentration remained constant in the coagulation bath, the variation in AgNP content was primarily influenced by the TA concentration.

The diffusion behavior of AgNPs within the membrane matrix can be attributed to two key mechanisms: (a) solvent and non-solvent diffusion and (b) the reduction of Ag^+ ions into AgNPs. Tannic acid regulates these processes, ultimately influencing the membranes' performance in oil/water separation applications. During phase inversion, a dense surface layer rapidly formed upon immersion of the thin film into the coagulation bath, driven by the rapid outward diffusion of the solvent.[53] As a hydrophilic agent, tannic acid facilitated the inward diffusion of

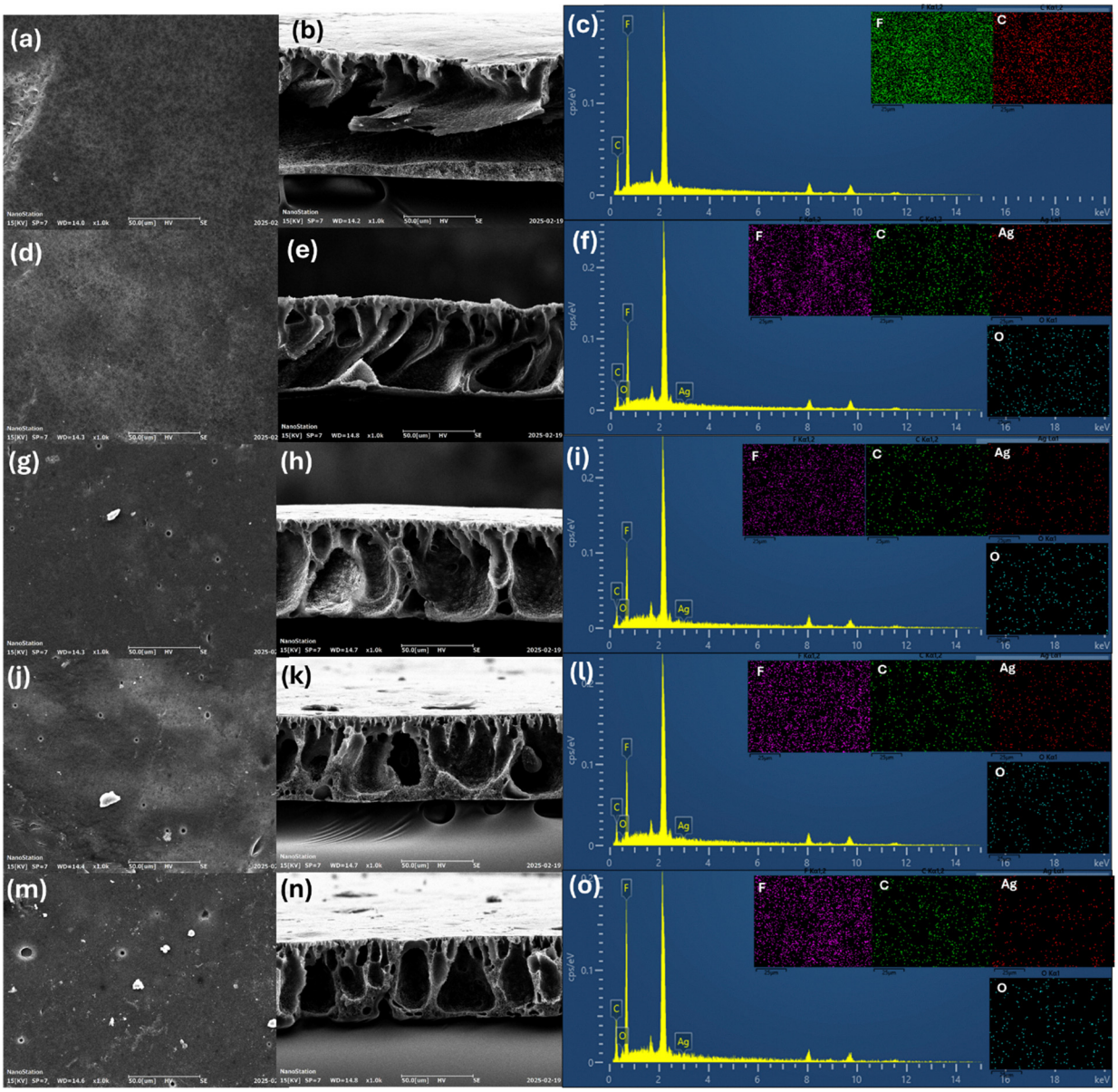

Fig. 2 SEM images of the surface and cross-section, along with EDX and elemental mapping of membranes: (a–c) M1, (d–f) M2, (g–i) M3, (j–l) M4, and (m–o) M5.

the non-solvent-containing Ag^+ ions. Consequently, higher TA concentrations enhanced non-solvent diffusion, promoting greater Ag^+ migration into the PVDF matrix. The subsequent reduction of Ag^+ to AgNPs by tannic acid further increased the Ag content within the membrane, explaining the observed rise in Ag weight percentage from 0.16% to 2.46% in M2–M5.

Additionally, at higher TA concentrations, reduced TA mobility led to a greater accumulation of AgNPs on the membrane surface. This was primarily attributed to hydrogen bonding interactions between TA and polyvinylpyrrolidone (PVP) in the casting solution, which induced agglomeration, preventing a homogeneous AgNP distribution across the membrane. While membranes with higher TA concentrations demonstrated enhanced antimicrobial properties for water treatment applications, their increased density potentially reduced permeability. This effect was later confirmed through permeability analysis of different membrane compositions. A higher loading of tannic acid, which consequently leads to an increased deposition of AgNPs, results in partial blockage of membrane pores. Although elevated tannic acid concentrations enhance the hydrophilicity of the membrane surface, they do not necessarily promote high permeability. This effect is particularly evident in the SEM surface images of the M4 and M5 membranes, where a significant reduction in surface porosity is observed (Fig. 2j and m). The densification of the membrane structure at higher tannic acid concentrations likely contributes to restricted water flow, thereby reducing overall permeability.

3.2. Physico-chemical characterization

ATR-FTIR was conducted to demonstrate the successful grafting of tannic acid and AgNPs on the PVDF membrane, and the result is shown in Fig. 3a. Compared with M1, the band at 1725 cm^{-1}, corresponding to the stretching vibration of the carboxyl group or ketone group of PVP increases with the increase in the concentration of TA from M-1 to M-5.[54] The characteristic band of the carboxyl group at 1725 cm^{-1} demonstrated the successful grafting of TA onto the PVDF membrane surface *via* the phase inversion method. The increase in intensity of the peak at 980 cm^{-1} with higher concentrations of TA indicates the presence of more C–O bonds, which are abundant in TA molecules.[55] This peak can also be attributed to the CH_2 rocking vibration in the α-phase of PVDF. The increase in intensity might suggest changes in the crystalline structure of PVDF due to interactions with tannic acid and AgNPs.[56] The increase in the intensity of C–H out of plane bending vibrations at around 750 cm^{-1} could be related to the presence of aromatic rings in tannic acid.[56]

Fig. 3b exhibits the surface charges of membranes with and without TA. Although the pristine M1 membrane surface is found to be negatively charged, after the infusion of TA, the surfaces were more negatively charged because of the phenolic hydroxyl groups in TA.[57] Interestingly, TA reduced silver ions by sacrificing some phenolic hydroxyl groups, the ζ potential of all modified surfaces did not change dramatically compared with that of the M1 membrane. All the membranes showed negative zeta potential at higher pH values due to deprotonation of the functional groups.[58–60] In addition, because the cell walls of microorganisms normally show negative charges, the modified surface may result in electrostatic repulsion interactions with bacteria; this is highly favorable to the formation of an anti-adhesive membrane surface.[61]

As shown in Fig. 3c, the contact angle of the M-1 membrane was 78.2° and reduced significantly to 53.9° for M-2 in the presence of TA. The abundance of phenolic hydrophilic functional groups in TA defined the increase in surface hydrophilicity.[62–64] This finding further validated the grafting of TA onto the membrane's surface. Upon Ag deposition and the subsequent increase in the capture of silver nanoparticles on the membrane, the contact was further reduced by 36.4°, 21.2°, and 15.2° for M-3, M-4, and M-5, respectively. This also confirmed that TA and PVP can significantly improve the hydrophilicity of the membranes. This was because the DMF solution inhibited the hydrogen bonding of TA and PVP, and

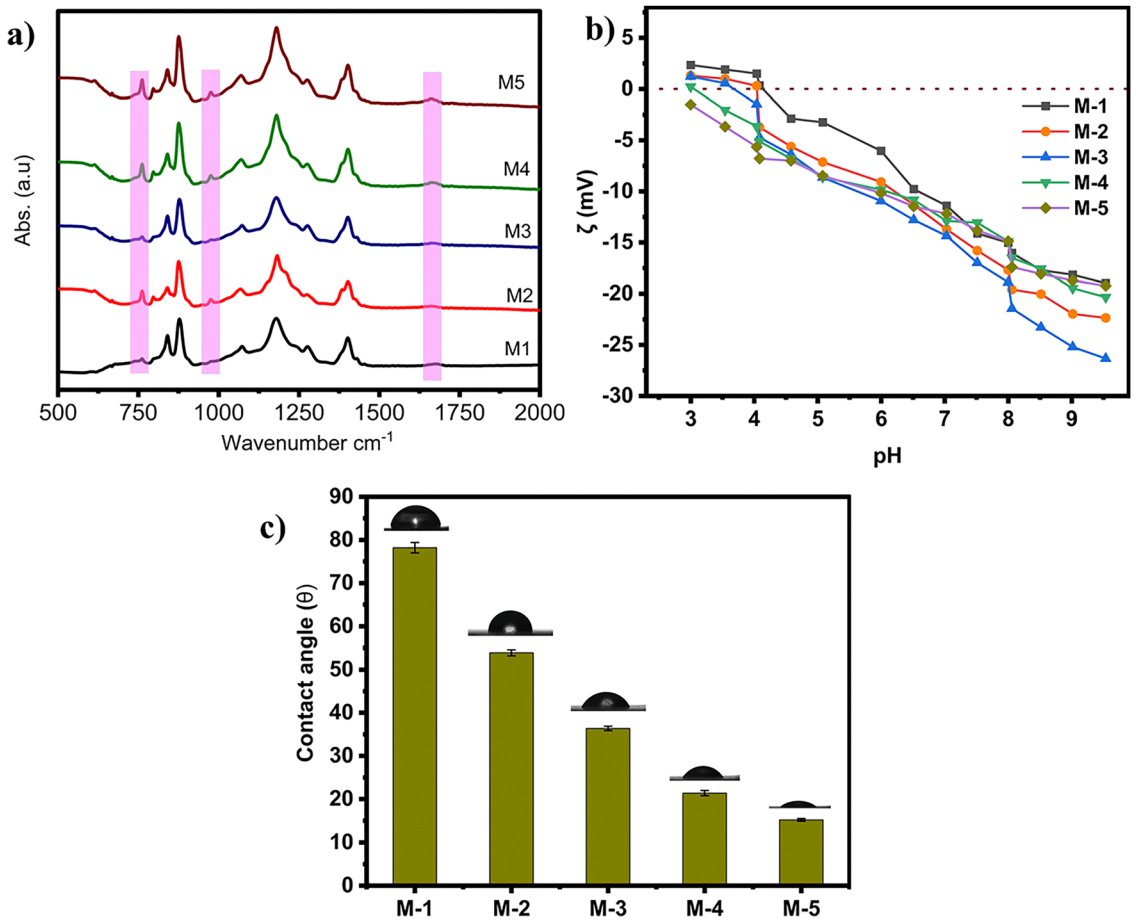

Fig. 3 Physico-chemical characterization of M1, M2, M3, M4, and M5. (a) ATR-FTIR spectra depicting changes in the bands and peak intensities from M1 to M5 with varying concentrations of TA. (b) Contact angle measurements showing a change of hydrophilicity values from M1 to M5. (c) Streaming potential analysis showing surface charge variation of membranes.

the polymer had an extended structure in the solution, allowing it to enter the microporous structure of the membrane and form a hydrophilic layer on the pore wall. The increase in concentration of TA, which results in the capture of more Ag particles, was clearly responsible for the enhanced hydrophilicity of the membrane surface. This property of membranes is a governing factor for anti-fouling behavior. The more hydrophilic a surface is, the less it will be prone to the deposition of foulants because of the formation of a strong hydration layer. The membrane surface will be easy to clean off and hence the flux recovery of the membrane will be significantly improved.[65,66]

3.3. Anti-bacterial test

As depicted in Fig. 4, the antibacterial activity of all the membranes was investigated using the disc diffusion method, a widely used technique for assessing antibacterial activity.[67] As anticipated, M1 did not demonstrate any action against Gram-negative bacteria (*E. coli*) as there were no identified inhibition zones, which are the areas between the radius of the pellicles and the distances of the bacterial colonies to the pellicle centers. However, the inhibition zone radius increased from M2 to M5, with M5 showing the highest inhibition zone at 3 mm. This was due to the fact that Ag^+ can strongly attract the sulfhydryl group (–SH) on the protease in the bacterial body, and binds rapidly to it, deactivating the protease and causing the death of the bacteria.[68] The PVDF membrane achieves excellent antibacterial properties due to the double bactericidal effect imparted by TA and silver ions.

The antibacterial functionality of the membrane is particularly advantageous for oil–water emulsion separation, as biofouling caused by bacterial colonization is a major challenge in membrane-based separation processes.[69] Bacterial growth on the membrane surface can lead to biofilm formation, reducing separation efficiency and shortening the membrane's lifespan.[70] The incorporation of Ag^+ ions and TA in the PVDF membrane provides an antibacterial barrier, effectively inhibiting bacterial adhesion and biofilm formation. This is achieved through the sustained release of Ag^+ ions, which disrupt bacterial cell membranes and interfere with metabolic processes, as well as the presence of TA, which further enhances antibacterial activity through its polyphenolic structure and ability to chelate metal ions.[71,72]

In aqueous medium with higher organic content such as oil–water emulsion, the membrane's antibacterial properties prevent the accumulation of biofilms, which can otherwise lead to pore blockage and reduced permeance. This is particularly important for maintaining consistent flux and rejection rates during prolonged operation. The antibacterial properties of the membrane also contribute to its self-cleaning ability, as the inhibition of bacterial growth prevents the formation of biofilms that can act as a scaffold for the deposition of oil droplets and other foulants.[71,73] This minimizes the need for frequent chemical cleaning or membrane replacement, thereby reducing operational costs and enhancing sustainability. This self-cleaning capability is crucial for maintaining high separation efficiency and prolonging the membrane's lifespan.[74]

3.4. Pure water flux and oil in water emulsion fouling

The pure water flux (PWF) and oil-in-water emulsion flux of the newly developed TA/AgNPs PVDF matrix membranes were

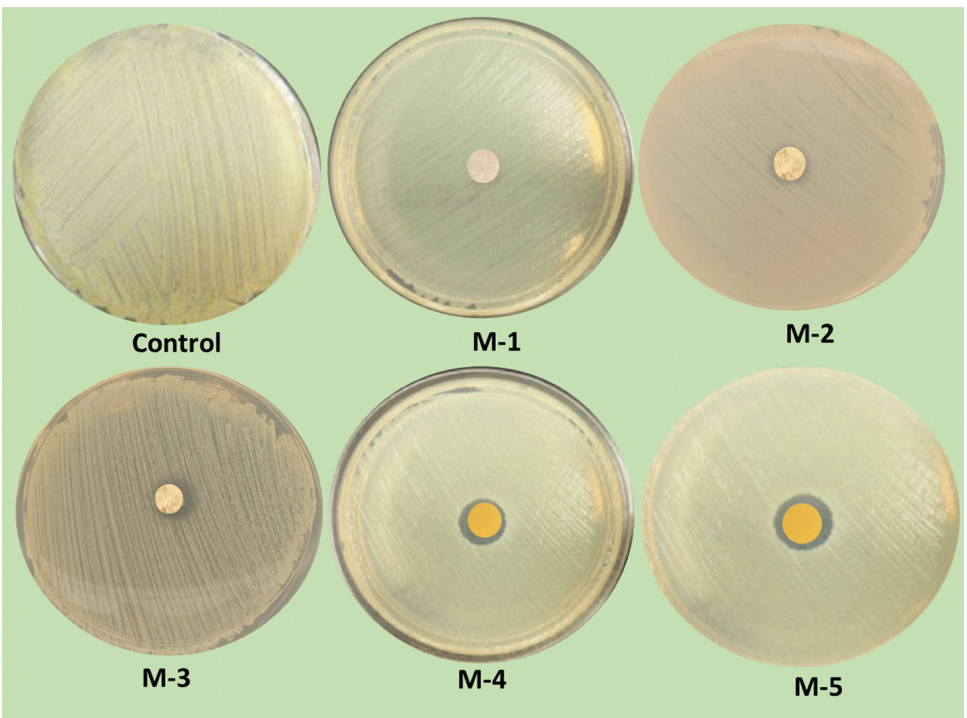

Fig. 4 Antibacterial test by the disk diffusion method. The growth of the inhibition zone from M1 to M5, with M1 having no inhibition zone and M5 showing the highest inhibition radius.

investigated under varying pressures, as depicted in Fig. 5. M2 and M3 demonstrated an increase in PWF because of the optimized pore structure and an increase in the number of pores by the pore-forming agent PVP. However, M3 and M5 exhibit reduced PWF compared to other membranes. This decline in flux can be attributed to the deposition of tannic acid, which significantly reduces the membrane porosity.[75] As the concentration of tannic acid increases, more AgNPs are captured within the membrane matrix, further blocking the pores. This pore obstruction substantially reduces the membrane's permeability, limiting the overall water flux even with the pressure increments. Also, during the reduction of silver ions, the Ag NPs formed near the pores tended to cover some areas of the pores in the case of M4 and M5; this might have led to a reduction in the pore diameter. SEM images also revealed a dense membrane surface for M4 and M5. At the same time, the elemental composition indicated a higher loading of AgNPs in the M4 and M5 membranes (Fig. 2). On the other hand, the improvement in the surface hydrophilicity in the case of M2 and M3 greatly outweighed the reduction in the pore size and resulted in an improvement in the water permeability of the modified membranes. Therefore, it was obvious that direct TA modification combined with the *in situ* formation of Ag NPs was feasible for the modification of membranes without sacrificing water performance at optimized concentrations of 0.2% and 0.4%. The PWF increases linearly with pressure; the best operating pressure was 2 bar. The rest of the fouling experiments were carried out at 2 bar.

The analysis of membrane performance for fouling resistance with diesel-in-water emulsions revealed interesting trends in flux decline and recovery across different membrane compositions. Membranes M1, M2, and M3 demonstrate relatively stable performance with moderate flux declines and good recovery rates, particularly M2 and M3, which show improved initial flux and better recovery compared to M1, indicating that low concentrations of TA enhance membrane performance likely due to improved hydrophilicity and antifouling properties.[76,77] However, a significant drop in performance is observed for M4 (0.6% tannic acid) and M5 (1% tannic acid), which exhibit much higher flux declines and lower flux recovery rates. Optical photographs of the oil-in-water separation of the optimum membrane are depicted in Fig. 8. The initial PWF for these membranes is also lower than that of M2 and M3, indicating reduced permeability. This decline in performance can be attributed to the higher TA content leading to pore closure and increased fouling during oil–water emulsion filtration. As the tannic acid content increases, there is a corresponding increase in the capture of silver AgNPs on the membrane surface, which enhances antibacterial activity. However, this comes at the cost of reduced flux and recovery rates. The mechanism behind this performance drop likely involves the interaction between tannic acid and the membrane structure; at higher concentrations, tannic acid may form a denser layer on the membrane surface and within the pores, leading to pore closure that reduces overall permeability, increased oil adhesion that heightens fouling susceptibility, and reduced cleaning efficiency due to altered

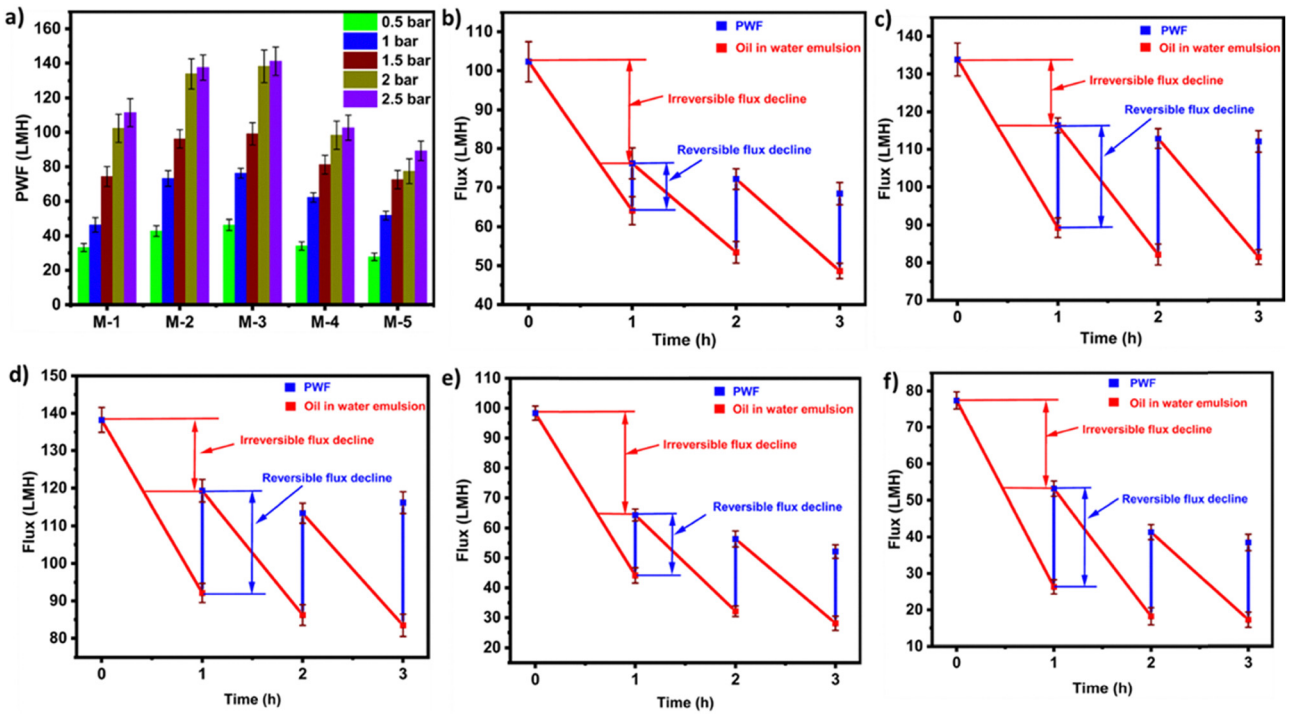

Fig. 5 PWF and fouling with oil in water emulsion for M1, M2, M3, M4 and M5. (a) PWF variation with pressure from 0.5 bar to 2.5 bar. (b) Reversible and irreversible flux decline for M1 with oil in water emulsion. (c) Reversible and irreversible flux decline for M2 with oil in water emulsion. (d) Reversible and irreversible flux decline for M3 with oil in water emulsion. (e) Reversible and irreversible flux decline for M4 with oil in water emulsion. (f) Reversible and irreversible flux decline for M5 with oil in water emulsion.

surface chemistry.[63,64] The flux declines, and the recovery rates for M4 and M5 support these hypotheses, as both membranes show significantly higher flux declines during oil–water emulsion filtration, 55.1% for M4 and 66% for M5 in the first cycle, compared to M1, M2, and M3. Additionally, their recovery rates are much lower, indicating persistent fouling that is not easily removed by washing. Over multiple cycles, this performance degradation becomes more pronounced; by the third cycle, M4 and M5 show alarmingly high flux declines of 71.4% and 77.8%, respectively, from their initial PWF, while M3 maintains relatively stable performance with only a 17.9% decline by the third cycle. This analysis suggests that there is an optimal concentration of tannic acid for enhancing membrane performance; low concentrations (0.2–0.4%) appear to improve hydrophilicity and antifouling properties without significantly compromising permeability, whereas higher concentrations (0.6% and above) lead to detrimental effects on membrane structure and function, resulting in severe performance degradation during oil–water separation (Fig. 6).

The average flux recovery values and oil rejection over three filtration cycles for membranes M1–M5 showed varying performance characteristics across different TA concentrations and cleaning methods. When using DI water for cleaning, M2 and M3 exhibited better flux recovery (85.1% and 84.12%, respectively) compared to M1 (70.5%), M4 (58.5%), and M5 (57.1%). This trend was further enhanced when using 0.05 M NaOH as the cleaning agent, with M2 and M3 showing even higher flux recovery (91.16% and 90.8%), while M1, M4, and M5 also saw slight improvements (73.63%, 60.86%, and 58.8%, respectively). The better flux recovery when NaOH was used as a cleaning solution can be attributed to its ability to saponify and emulsify oil foulants, as well as its capacity to modify the surface charge of the membrane, leading to decreased adhesion between the membrane and foulants.[78] Although no apparent change was observed during NaOH cleaning, alternative cleaning agents should be explored to ensure minimal impact on the structural integrity of the PVDF membranes.[79] The oil-in-water emulsion rejection for all membranes except M1 demonstrated high efficiency, with M5 showing the highest rejection at 95%, followed closely by M2 (93%), M3 (92%), and M4 (91%). However, it's crucial to note that while M4 and M5 exhibited higher oil rejection, they were more susceptible to fouling and showed significantly lower flux recovery rates. This suggests that the increased TA concentration in these

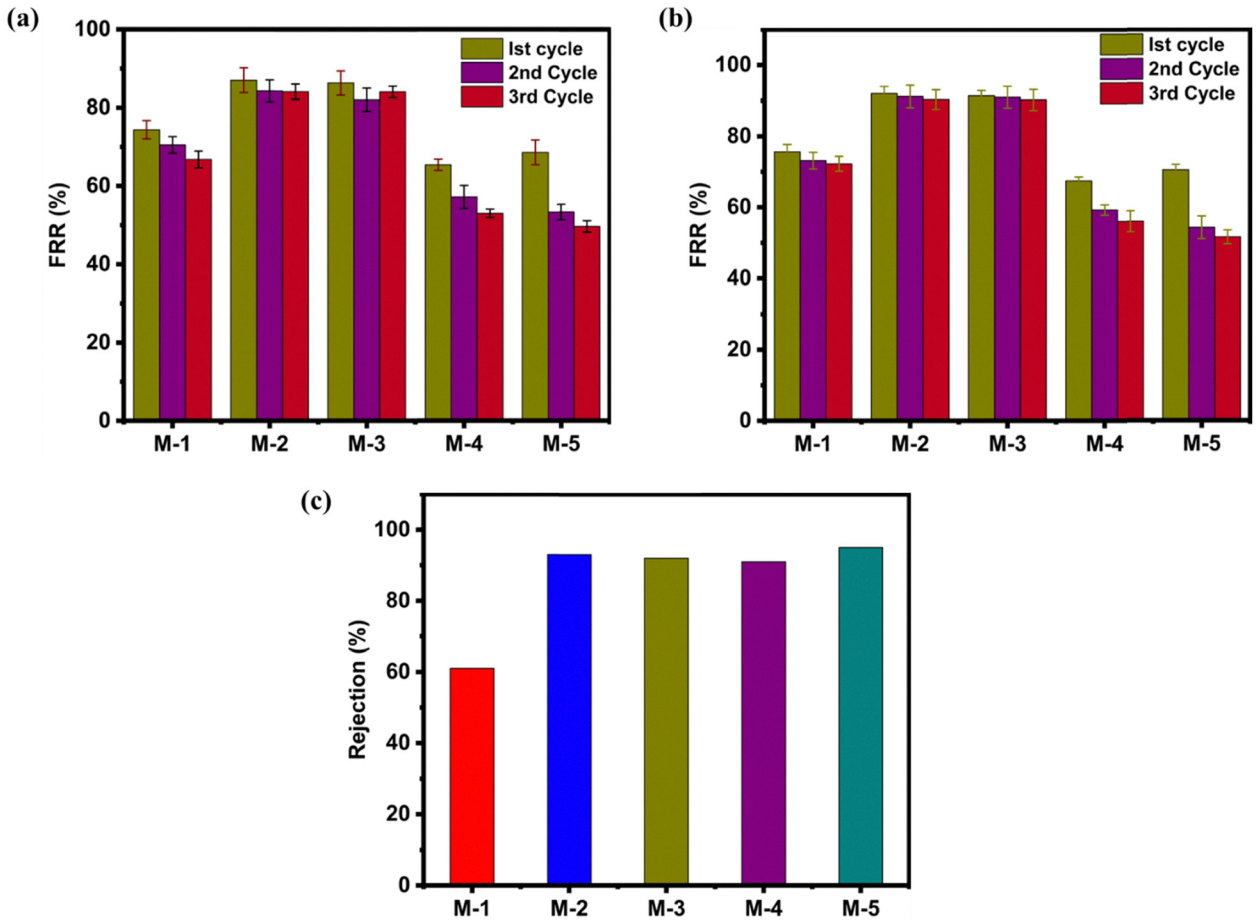

Fig. 6 Flux recovery and rejection of diesel-in-water emulsions for M1, M2, M3, M4 and M5. (a) Flux recovery ratio (%) over three cycles of filtration when DI water was used as a cleaning agent. (b) Flux recovery ratio (%) over three cycles of filtration when 0.05 M NaOH water was used as a cleaning agent. (c) Rejection (%) of NOM measured in terms of total organic carbon analysis.

membranes, enhancing oil rejection through increased hydrophilicity and possibly smaller pore sizes, also led to more persistent fouling and reduced permeability. In contrast, M2 and M3 achieved an optimal balance, demonstrating high oil rejection (93% and 92%) while maintaining excellent flux recovery, indicating better antifouling properties and overall performance.

3.5. Organic fouling tests with NOM

From the fouling tests with the oil-in-water emulsion, the best-performing membranes M1, M2, and M3 were further evaluated for a complex organic foulant stream named NOM. The evaluation of membranes M1, M2, and M3 for fouling resistance using a synthetic NOM solution revealed performance trends similar to those observed in oil–water emulsion tests. M2 and M3 demonstrated better flux recovery and NOM rejection than M1, highlighting their enhanced antifouling properties. The average flux recovery percentages for M1, M2, and M3 were 64%, 87%, and 85%, respectively, while the NOM rejection rates were 66%, 86%, and 91%. These results indicate that the membranes, particularly M2 and M3, exhibited excellent recovery and rejection capabilities even with complex foulant solutions. The improved performance of M2 and M3 can be attributed to the optimal concentration of tannic acid, which likely enhances surface hydrophilicity and creates a more effective antifouling barrier.[77,80] The literature reports that hydrophilic surfaces typically contribute to forming a strong hydration layer, which enhances fouling resistance.[81,82] Tannic acid is rich in hydrophilic groups, such as hydroxyl and ester linkages. The hydroxyl groups, in particular, facilitate the formation of a hydration layer through hydrogen bonding with water, thereby preventing foulant adhesion to the membrane surface. This performance surpasses several studies reported, such as polyethersulfone ultrafiltration membranes, which showed a maximum flux recovery of 71.2% with humic acid fouling.[83] Similarly, a study reported a flux recovery of 76.3% for polyvinylidene fluoride membranes modified with graphene oxide in NOM filtration.[84] Another study reported a maximum flux recovery of 80% with polyethersulfone membranes incorporating TiO_2 nanoparticles for NOM removal.[85] The limitations in these studies often stem from surface modification or suboptimal hydrophilicity balance. Furthermore, a study reported NOM rejection of 85% for their best-performing membrane, which falls short of the 91% achieved by M3 in the current study.[48] Also, Liu *et al.* demonstrated a flux recovery of 82.5% with their modified polysulfone membranes in NOM filtration, which is lower than the performance of M2 and M3.[86] The superior performance of M2 and M3 in the present study underscores the effectiveness of TA modification in creating membranes with exceptional fouling

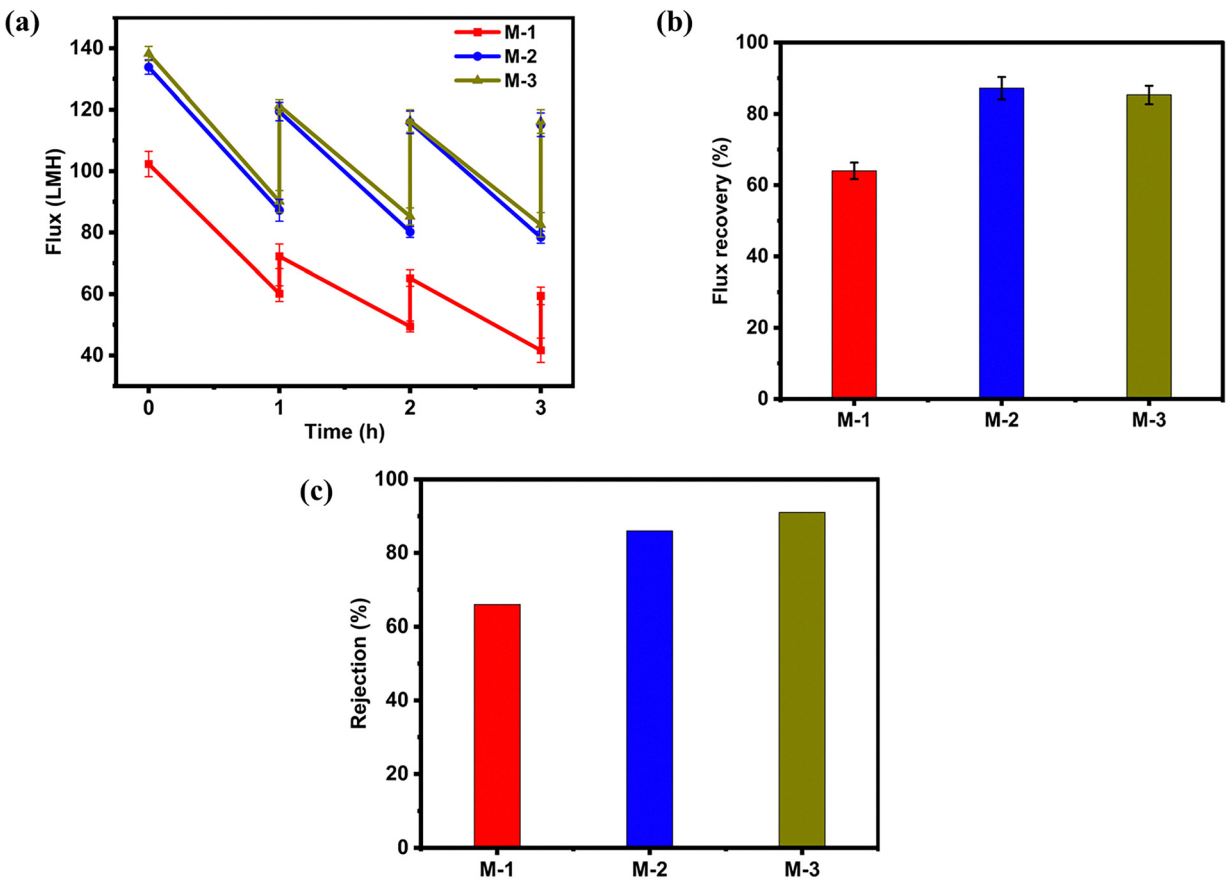

Fig. 7 Membrane performance with synthetic NOM for M1, M2 and M3. (a) Flux decline and recovery profile over three filtration cycles for M1, M2 and M3. (b) Average flux recovery ratio (%) measured over three filtration cycles. (c) Rejection of NOM measured as the organic carbon content analysis.

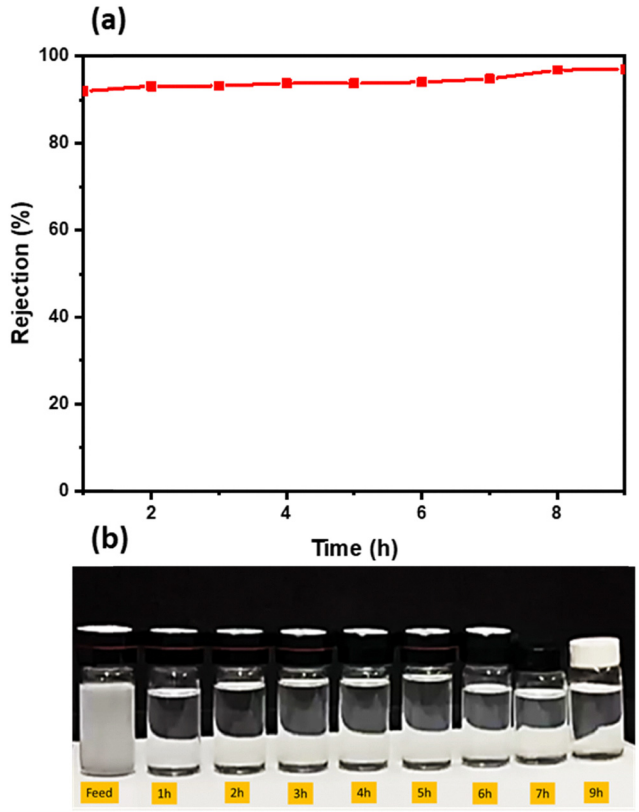

Fig. 8 (a) Long-term operational stability of the M3 membrane during the separation of an oil-in-water emulsion using a cross-flow filtration system. (b) Image of the feed and permeate collected at different intervals.

resistance and NOM rejection capabilities, potentially opening new avenues for advanced and fouling-resistant membrane materials (Fig. 7).

The M2 and M3 membranes demonstrated the best overall performance in terms of rejection efficiency, permeability, and resistance to fouling. Among them, the M3 membrane was selected for further evaluation, focusing on its leaching behavior and long-term operational stability.

Ag was incorporated *in situ* into the membrane matrix with the assistance of TA, and its leaching potential was assessed using ICP-OES. The M3 membrane was operated for 1 hour, after which the permeate was collected and analyzed *via* ICP-OES. The results indicated that Ag leaching was below the detection limit, confirming the stable integration of silver within the membrane matrix.

To assess long-term performance, the separation efficiency of the M3 membrane was continuously monitored over a 9-hour operation in a cross-flow filtration system. Throughout this period, the membrane consistently maintained high rejection rates, ranging from 92% to 97% (Fig. 8a). The camera captured images of the feed and the permeate at different intervals, as shown in Fig. 8b. A slight increase in rejection was observed over time, likely due to the gradual accumulation of foulants on the membrane surface, which may have enhanced the barrier properties.

To compare the performance of the newly developed TA-AgNPs-PVDF membranes for oil-in-water emulsion separation, Table 2 presents a comprehensive comparison of their flux and rejection capabilities against other reported membrane materials in the literature.

4. Conclusion

This comprehensive study investigated the development and performance of PVDF membranes modified with varying concentrations of TA and AgNPs for enhanced fouling resistance for oil–water separation and natural organic matter (NOM) filtration. This study explored incorporating varied concentrations of TA (0% to 1%) to capture AgNPs from $AgNO_3$ in the

Table 2 Comparison of TA-AgNPs-PVDF membranes against other explored membranes in the literature

Membrane material	Flux (L m^{-2} h^{-1} bar^{-1})	Oil in water emulsion rejection (%)	Ref.
Commercial PVDF	<200	<90	87
PES/cellulose acetate/chitosan	70	98.2–99.5	88
CA–GO composite	45.2	80.1–90.3	89
CA-bentonite composite	53.4	75.0–95.0	89
CA–TiO_2 composite	100.3	90.3–95.2	89
Polystyrene + Al_2O_3 nanoparticles	146	97.5–97.9	90
Polyamide 66/α-alumina composite	10–30	78.5–99.5	91
PES (commercial UF, MT)	87.4	97	91
PES (commercial UF, XT)	64.0	100	91
PES (commercial NF, NFS)	10.1	99	91
PES (commercial NF, NFX)	10.1	95	91
PA TFC (FILMTEC)	45.8	98	91
PA (GC)	26.1	100	91
Alumina (Al_2O_3)	20–50	90–95	92
SiC-deposited alumina	30–60	95–98	92
Poly(trimethyl hexamethylene terephthalamide)	10–60	4–85	93
Modified ceramic (eggshell, starch)	<100	90–95	94
PES + PVP	10–70	79–98	95
PES + bentonite	112–612	90–95	96
PVDF + grafted short chain alkylamines	3–100	60–98	97
TA-AgNPs-PVDF (M2/M3)	**~300–400**	**92–93**	**This work**

coagulation bath. The morphology of the membranes revealed that higher TA content led to increased capture of silver nanoparticles, enhancing the membranes' antibacterial properties. Performance evaluation using oil–water emulsions and NOM solutions demonstrated that membranes M2 and M3, with 0.2% and 0.4% tannic acid, respectively, achieved an optimal balance between flux performance, fouling resistance, and contaminant rejection. These membranes exhibited superior flux recovery rates (up to 91.16% with NaOH cleaning) and high rejection efficiencies for both oil and NOM. In contrast, despite high rejection rates, M4 and M5 membranes, with higher tannic acid concentrations, showed increased fouling susceptibility and reduced flux recovery. This study also highlighted the effectiveness of 0.05 M NaOH as a cleaning agent, significantly improving flux recovery compared to DI water. Overall, the research demonstrated that carefully optimized tannic acid modification can significantly enhance membrane performance in complex water treatment applications, surpassing several benchmarks reported in the literature.

Future research could further optimize the tannic acid concentration and investigate these membranes' long-term stability and performance under various operating conditions and with different contaminants.

Conflicts of interest

There are no conflicts to declare.

Data availability

The data will be available from the authors on reasonable request.

Acknowledgements

Support for this work provided by Nazarbayev University under the Collaborative Research Project Grant (Grant No. 111024CRP2017) and the Faculty Development Competitive Research Grant Programs (Grant No. 040225FD4729) is gratefully acknowledged. The authors would also like to acknowledge the support provided by the IRC-MWS at King Fahd University of Petroleum and Minerals (KFUPM).

References

1 D. S. Mallya, L. F. Dumée, S. Muthukumaran, W. Lei and K. Baskaran, 2D Nanosheet Enabled Thin Film Nanocomposite Membranes for Freshwater Production – a Review, *Mater Adv.*, 2021, **2**(11), 3519–3537, DOI: **10.1039/D1MA00256B**.

2 M. D. Islam, F. J. Uddin, T. U. Rashid and M. Shahruzzaman, Cellulose Acetate-Based Membrane for Wastewater Treatment—A State-of-the-Art Review, *Mater Adv.*, 2023, **4**(18), 4054–4102, DOI: **10.1039/D3MA00255A**.

3 M. R. Rahman, A. James, K. A. M. Said, M. Namakka, M. U. Khandaker, W. H. Jiunn, J. Y. Al-Humaidi, R. H. Althomali and M. M. Rahman, A TiO_2 Grafted Bamboo Derivative Nanocellulose Polyvinylidene Fluoride (PVDF) Nanocomposite Membrane for Wastewater Treatment by a Photocatalytic Process, *Mater Adv.*, 2024, **5**(19), 7617–7636, DOI: **10.1039/D4MA00716F**.

4 A. Zahid, H. H. Nawaz, A. Siddique, B. Ahmed, S. Razzaque, X. Liu, H. Razzaq and M. Umar, Enabling Improved PSF Nanocomposite Membrane for Wastewater Treatment with Selective Nanotubular Morphology of PANI/ZnO, *Mater. Adv.*, 2024, **5**(23), 9471–9487, DOI: **10.1039/D4MA00859F**.

5 H. C. Kim, B. G. Choi, J. Noh, K. G. Song, S. Hyup Lee and S. K. Maeng, Electrospun Nanofibrous PVDF-PMMA MF Membrane in Laboratory and Pilot-Scale Study Treating Wastewater from Seoul Zoo, *Desalination*, 2014, **346**, 107–114, DOI: **10.1016/j.desal.2014.05.005**.

6 L. Cheng, L. Li, X. Pei, Y. Ma, F. Liu and J. Li, PVDF/MOFs Mixed Matrix Ultrafiltration Membrane for Efficient Water Treatment, *Front Chem.*, 2022, **10**, 985750, DOI: **10.3389/fchem.2022.985750**.

7 F. Liu, N. A. Hashim, Y. Liu, M. R. M. Abed and K. Li, Progress in the Production and Modification of PVDF Membranes, *J. Membr. Sci.*, 2011, **375**(1–2), 1–27, DOI: **10.1016/j.memsci.2011.03.014**.

8 S. Yang, D. Yang, W. Ren, J. Liu, J. Mou and Y. Wang, Analysis of Research Status of Modified PVDF Ultrafiltration Membrane, *IOP Conf. Ser.: Earth Environ. Sci.*, 2020, **585**, DOI: **10.1088/1755-1315/585/1/012190**.

9 J. Zhang, Z. Xu, W. Mai, C. Min, B. Zhou, M. Shan, Y. Li, C. Yang, Z. Wang and X. Qian, Improved Hydrophilicity, Permeability, Antifouling and Mechanical Performance of PVDF Composite Ultrafiltration Membranes Tailored by Oxidized Low-Dimensional Carbon Nanomaterials, *J. Mater. Chem. A*, 2013, **1**(9), 3101–3111, DOI: **10.1039/c2ta01415g**.

10 Y. Zhang, L. Ye, B. Zhang, Y. Chen, W. Zhao, G. Yang, J. Wang and H. Zhang, Characteristics and Performance of PVDF Membrane Prepared by Using NaCl Coagulation Bath: Relationship between Membrane Polymorphous Structure and Organic Fouling, *J. Membr. Sci.*, 2019, **579**, 22–32, DOI: **10.1016/j.memsci.2019.02.054**.

11 L. Shen, S. Feng, J. Li, J. Chen, F. Li, H. Lin and G. Yu, Surface Modification of Polyvinylidene Fluoride (PVDF) Membrane via Radiation Grafting: Novel Mechanisms Underlying the Interesting Enhanced Membrane Performance, *Sci. Rep.*, 2017, **7**(1), 2721, DOI: **10.1038/s41598-017-02605-3**.

12 A. Gul, J. Hruza and F. Yalcinkaya, Fouling and Chemical Cleaning of Microfiltration Membranes: A Mini-Review, *Polymers*, 2021, **13**(6), 846, DOI: **10.3390/polym13060846**.

13 E. M. Vrijenhoek, S. Hong and M. Elimelech, Influence of Membrane Surface Properties on Initial Rate of Colloidal Fouling of Reverse Osmosis and Nanofiltration Membranes, *J. Membr. Sci.*, 2001, **188**(1), 115–128, DOI: **10.1016/S0376-7388(01)00376-3**.

14 F. Meng, S. R. Chae, A. Drews, M. Kraume, H. S. Shin and F. Yang, Recent Advances in Membrane Bioreactors (MBRs):

Membrane Fouling and Membrane Material, *Water Res.*, 2009, **43**(6), 1489–1512, DOI: 10.1016/j.watres.2008.12.044.

15 N. Alsawaftah, W. Abuwatfa, N. Darwish and G. Husseini, A Comprehensive Review on Membrane Fouling: Mathematical Modelling, Prediction, Diagnosis, and Mitigation, *Water*, 2021, **13**(9), 1327, DOI: 10.3390/w13091327.

16 S. Jiang, Y. Li and B. P. Ladewig, A Review of Reverse Osmosis Membrane Fouling and Control Strategies, *Sci. Total Environ.*, 2017, **595**, 567–583, DOI: 10.1016/j.scitotenv.2017.03.235.

17 H. K. Lee, W. Kim, Y. M. Kim and Y. N. Kwon, Surface Modification of Polyvinylidene Fluoride Membrane for Enhanced Wetting Resistance, *Appl. Surf. Sci.*, 2019, **491**, 32–42, DOI: 10.1016/j.apsusc.2019.06.135.

18 G. Dong Kang and Y. Ming Cao, Application and Modification of Poly(Vinylidene Fluoride) (PVDF) Membranes - A Review, *J. Membr. Sci.*, 2014, **463**, 145–165, DOI: 10.1016/j.memsci.2014.03.055.

19 S. M. Saleh, P. C. Oh and A. S. Zulkifli, Surface Modification of PVDF Membrane via Graft Polymerization of Acetic and Acrylic Acid, *IOP Conf. Ser. Mater. Sci. Eng.*, 2022, **1257**(1), DOI: 10.1088/1757-899x/1257/1/012032.

20 S. Shen, Y. Shen, Y. Wu, H. Li, C. Sun, G. Zhang and Y. Guo, Surface Modification of PVDF Membrane via Deposition-Grafting of UiO-66-NH2 and Their Application in Oily Water Separations, *Chem. Eng. Sci.*, 2022, **260**, 117934, DOI: 10.1016/j.ces.2022.117934.

21 C. Liu, L. Wu, C. Zhang, W. Chen and S. Luo, Surface Hydrophilic Modification of PVDF Membranes by Trace Amounts of Tannin and Polyethyleneimine, *Appl. Surf. Sci.*, 2018, **457**, 695–704, DOI: 10.1016/j.apsusc.2018.06.131.

22 H. Zheng, M. Zhu, D. Wang, Y. Zhou, X. Sun, S. Jiang, M. Li, C. Xiao, D. Zhang and L. Zhang, Surface Modification of PVDF Membrane by CNC/Cu-MOF-74 for Enhancing Antifouling Property, *Sep. Purif. Technol.*, 2023, **306**, 122599, DOI: 10.1016/j.seppur.2022.122599.

23 L. Shen, S. Feng, J. Li, J. Chen, F. Li, H. Lin and G. Yu, Surface Modification of Polyvinylidene Fluoride (PVDF) Membrane via Radiation Grafting: Novel Mechanisms Underlying the Interesting Enhanced Membrane Performance, *Sci. Rep.*, 2017, **7**(1), DOI: 10.1038/s41598-017-02605-3.

24 X. Zhang, Y. Wang, Y. Liu, J. Xu, Y. Han and X. Xu, Preparation, Performances of PVDF/ZnO Hybrid Membranes and Their Applications in the Removal of Copper Ions, *Appl. Surf. Sci.*, 2014, **316**(1), 333–340, DOI: 10.1016/j.apsusc.2014.08.004.

25 T. M. H. Le, R. Wang and S. Sairiam, Self-Protecting PVDF-PDA-TiO2 Membranes towards Highly Efficient and Prolonged Dye Wastewater Treatment by Photocatalytic Membranes, *J. Membr. Sci.*, 2023, **683**, 121789, DOI: 10.1016/j.memsci.2023.121789.

26 Y. Zhang, X. Duan, B. Tan, Y. Jiang, Y. Wang and T. Qi, PVDF Microfiltration Membranes Modified with AgNPs/Tannic Acid for Efficient Separation of Oil and Water Emulsions, *Colloids Surf., A*, 2022, **644**, 128844, DOI: 10.1016/j.colsurfa.2022.128844.

27 C. Zhao, N. S. Nguyen, X. Li, D. McCarthy and H. Wang, Tannic Acid Coating and in Situ Deposition of Silver Nanoparticles to Improve the Antifouling Properties of an Ultrafiltration Membrane, *J. Appl. Polym. Sci.*, 2019, **136**(14), 47314, DOI: 10.1002/app.47314.

28 Y. C. Lin, C. M. Chao, D. K. Wang, K. M. Liu and H. H. Tseng, Enhancing the Antifouling Properties of a PVDF Membrane for Protein Separation by Grafting Branch-like Zwitterions via a Novel Amphiphilic SMA-HEA Linker, *J. Membr. Sci.*, 2021, **624**, 119126, DOI: 10.1016/j.memsci.2021.119126.

29 N. Ma, J. Cao, H. Li, Y. Zhang, H. Wang and J. Meng, Surface Grafting of Zwitterionic and PEGylated Cross-Linked Polymers toward PVDF Membranes with Ultralow Protein Adsorption, *Polymer*, 2019, **167**, 1–12, DOI: 10.1016/j.polymer.2019.01.053.

30 L. Han, Y. Z. Tan, C. Xu, T. Xiao, T. A. Trinh and J. W. Chew, Zwitterionic Grafting of Sulfobetaine Methacrylate (SBMA) on Hydrophobic PVDF Membranes for Enhanced Anti-Fouling and Anti-Wetting in the Membrane Distillation of Oil Emulsions, *J. Membr. Sci.*, 2019, **588**, 117196, DOI: 10.1016/j.memsci.2019.117196.

31 S. A. Mousa, H. Abdallah, S. S. Ibrahim and S. A. Khairy, Enhanced photocatalytic properties of graphene oxide/polyvinylchloride membranes by incorporation with green prepared SnO2 and TiO2 nanocomposite for water treatment, *Appl. Phys. A: Mater. Sci. Process.*, 2023, **129**, 831, DOI: 10.1007/s00339-023-07117-8.

32 A. T. Lawal, Graphene-based nano composites and their applications: A review, *Biosens. Bioelectron.*, 2019, **141**, 111384, DOI: 10.1016/j.bios.2019.111384.

33 X. Li, A. Sotto, J. Li and B. Van der Bruggen, Progress and perspectives for synthesis of sustainable antifouling composite membranes containing in situ generated nanoparticles, *J. Membr. Sci.*, 2017, **524**, 502–528, DOI: 10.1016/j.memsci.2016.11.040.

34 Z. Yang, X. Zhang, M. Xie, H.-C. Wu, T. Yoshioka, D. Saeki and H. Matsuyama, Antifouling thin-film composite membranes with multi-defense properties by controllably constructing amphiphilic diblock copolymer brush layer, *J. Membr. Sci.*, 2020, **614**, 118515, DOI: 10.1016/j.memsci.2020.118515.

35 P. Karami, S. A. Aktij, B. Khorshidi, M. D. Firouzjaei, A. Asad, M. Elliott, A. Rahimpour, J. B. P. Soares and M. Sadrzadeh, Nanodiamond-decorated thin film composite membranes with antifouling and antibacterial properties, *Desalination*, 2022, **522**, 115436, DOI: 10.1016/j.desal.2021.115436.

36 O. Heinz, M. Aghajani, A. R. Greenberg and Y. Ding, Surface-patterning of polymeric membranes: Fabrication and performance, *Curr. Opin. Chem. Eng.*, 2018, **20**, 1–12, DOI: 10.1016/j.coche.2018.01.008.

37 N. U. Barambu, M. R. Bilad, Y. Wibisono, J. Jaafar, T. M. I. Mahlia and A. L. Khan, Membrane surface patterning as a fouling mitigation strategy in liquid filtration: A review, *Polymers*, 2019, **11**, 1687, DOI: 10.3390/polym11101687.

38 J. Xu, K. Guan, P. Luo, S. He, H. Matsuyama, D. Zou and Z. Zhong, Engineering PVDF omniphobic membranes with flower-like micro-nano structures for robust membrane distillation, *Desalination*, 2024, **578**, 117442, DOI: 10.1016/j.desal.2024.117442.

39 A. Ilyas, L. Timmermans, M. Vanierschot, I. Smets and I. F. J. Vankelecom, Micro-patterned PVDF membranes and magnetically induced membrane vibration system for efficient membrane bioreactor operation, *J. Membr. Sci.*, 2022, **662**, 120978, DOI: 10.1016/j.memsci.2022.120978.

40 H. Li, Y. Luo, F. Yu and H. Zhang, In-situ construction of MOFs-based superhydrophobic/superoleophilic coating on filter paper with self-cleaning and antibacterial activity for efficient oil/water separation, *Colloids Surf., A*, 2021, **625**, 126976, DOI: 10.1016/j.colsurfa.2021.126976.

41 Z. Yin, F. Yuan, M. Xue, Y. Xue, Y. Xie, J. Ou, Y. Luo, Z. Hong and C. Xie, A multifunctional and environmentally safe superhydrophobic membrane with superior oil/water separation, photocatalytic degradation and anti-biofouling performance, *J. Colloids Interface Sci.*, 2022, **611**, 93–104, DOI: 10.1016/j.jcis.2021.12.070.

42 S. Kang, M. Herzberg, D. F. Rodrigues and M. Elimelech, Antibacterial effects of carbon nanotubes: Size does matter, *Langmuir*, 2008, **24**, 6409–6413, DOI: 10.1021/la800951v.

43 B. Z. Ristic, M. M. Milenkovic, I. R. Dakic, B. M. Todorovic-Markovic, M. S. Milosavljevic, M. D. Budimir, V. G. Paunovic, M. D. Dramicanin, Z. M. Markovic and V. S. Trajkovic, Photodynamic antibacterial effect of graphene quantum dots, *Biomaterials*, 2014, **35**, 4428–4435, DOI: 10.1016/j.biomaterials.2014.02.014.

44 G. Applerot, J. Lellouche, N. Perkas, Y. Nitzan, A. Gedanken and E. Banin, ZnO nanoparticle-coated surfaces inhibit bacterial biofilm formation and increase antibiotic susceptibility, *RSC Adv.*, 2012, **2**, 2314–2321, DOI: 10.1039/c2ra00602b.

45 R. Verma, V. B. Chaudhary, L. Nain and A. K. Srivastava, Antibacterial characteristics of TiO2 nano-objects and their interaction with biofilm, *Mater. Technol.*, 2017, **32**, 385–390, DOI: 10.1080/10667857.2016.1236515.

46 L. Liu, C. Ge, Y. Zhang, W. Ma, X. Su, L. Chen, S. Li, L. Wang, X. Mu and Y. Xu, Tannic acid-modified silver nanoparticles for enhancing anti-biofilm activities and modulating biofilm formation, *Biomater. Sci.*, 2020, **8**, 4852–4860, DOI: 10.1039/d0bm00648c.

47 N. Baig, I. Abdulazeez, N. A. Khan and M. B. Hanif, Experimental and theoretical assessment of bioinspired next-generation intercalated graphene oxide-based ceramic membranes for oil-in-water emulsion separation, *npj Clean Water*, 2024, **7**, 82, DOI: 10.1038/s41545-024-00369-8.

48 P. Orlowski, M. Zmigrodzka, E. Tomaszewska, K. Ranoszek-Soliwoda, M. Czupryn, M. Antos-Bielska, J. Szemraj, G. Celichowski, J. Grobelny and M. Krzyzowska, Tannic acid-modified silver nanoparticles for wound healing: The importance of size, *Int. J. Nanomed.*, 2018, **13**, 991–1007, DOI: 10.2147/ijn.S154797.

49 D. Raghunandan, S. Basavaraja, B. Mahesh, S. Balaji, S. Y. Manjunath and A. Venkataraman, Biosynthesis of stable polyshaped gold nanoparticles from microwave-exposed aqueous extracellular anti-malignant guava (Psidium guajava) leaf extract, *Nanobiotechnology*, 2009, **5**, 34–41, DOI: 10.1007/s12030-009-9030-8.

50 H. Strathmann, Synthetic membranes and their preparation, *Springer Ebooks*, 1986, pp. 1–37. , DOI: 10.1007/978-94-009-4712-2_1.

51 K. Kimmerle and H. Strathmann, Analysis of the structure-determining process of phase inversion membranes, *Desalination*, 1990, **79**, 283–302, DOI: 10.1016/0011-9164(90)85012-Y.

52 Y. Tang, Y. Lin, D. M. Ford, X. Qian, M. R. Cervellere, P. C. Millett and X. Wang, A review on models and simulations of membrane formation via phase inversion processes, *J. Membr. Sci.*, 2021, **640**, 119810, DOI: 10.1016/j.memsci.2021.119810.

53 N. Baig, Z. Arshad and S. A. Ali, Synthesis of a biomimetic zwitterionic pentapolymer to fabricate high-performance PVDF membranes for efficient separation of oil-in-water nano-emulsions, *Sci. Rep.*, 2022, **12**, 5028, DOI: 10.1038/s41598-022-09046-7.

54 D. Liu, Y. Chen, T. T. Tran and G. Zhang, Facile and rapid assembly of high-performance tannic acid thin-film nanofiltration membranes via Fe3+ intermediated regulation and coordination, *Sep. Purif. Technol.*, 2021, **260**, 118228, DOI: 10.1016/j.seppur.2020.118228.

55 T. Wahyono, D. A. Astuti, I. K. Gede Wiryawan, I. Sugoro and A. Jayanegara, Fourier Transform Mid-Infrared (FTIR) spectroscopy to identify tannin compounds in the panicle of sorghum mutant lines, *IOP Conf. Ser.: Mater. Sci. Eng.*, 2019, **546**, 042045, DOI: 10.1088/1757-899X/546/4/042045.

56 L. Shen, S. Feng, J. Li, J. Chen, F. Li, H. Lin and G. Yu, Surface modification of polyvinylidene fluoride (PVDF) membrane via radiation grafting: Novel mechanisms underlying the interesting enhanced membrane performance, *Sci. Rep.*, 2017, **7**, 2721, DOI: 10.1038/s41598-017-02605-3.

57 M. Pourmadadi, Z. Omrani, R. Abbasi, M. Mirshafiei and F. Yazdian, Poly (tannic acid) based nanocomposite as a promising potential in biomedical applications, *J. Drug Delivery Sci. Technol.*, 2024, **95**, 105568, DOI: 10.1016/j.jddst.2024.105568.

58 A. Serrano-Lotina, R. Portela, P. Baeza, V. Alcolea-Rodriguez, M. Villarroel and P. Ávila, Zeta potential as a tool for functional materials development, *Catal. Today*, 2023, **423**, 113862, DOI: 10.1016/j.cattod.2022.08.004.

59 X. Tong, S. Liu, D. Qu, H. Gao, L. Yan, Y. Chen and J. Crittenden, Tannic acid-metal complex modified MXene membrane for contaminants removal from water, *J. Membr. Sci.*, 2021, **622**, 119042, DOI: 10.1016/j.memsci.2020.119042.

60 O. T. Mahlangu and B. B. Mamba, Interdependence of contributing factors governing dead-end fouling of nanofiltration membranes, *Membranes*, 2021, **11**, 47, DOI: 10.3390/membranes11010047.

61 L. Liu, Y. Liu, X. Chen, S. Feng, Y. Wan, H. Lu and J. Luo, *J. Membr. Sci.*, 2023, **668**, 121205, DOI: 10.1016/j.memsci.2022.121205.

62 S. Mallakpour and E. Azadi, Novel methodologies and materials for facile fabrication of nanofiltration

membranes, *Emergent Mater.*, 2022, **5**, 1288, DOI: **10.1007/s42247-021-00278-3**.

63 S. Zhou, Y. Qu, B. Yang, Q. Zhang, J. Wang, Y. Lin, Z. Chen and G. P. Lu, Bio-based tannic acid as a raw material for membrane surface modification, *Desalination*, 2023, **555**, 116535, DOI: **10.1016/j.desal.2023.116535**.

64 W. Yan, M. Shi, C. Dong, L. Liu and C. Gao, Applications of tannic acid in membrane technologies: A review, *Adv. Colloid Interface Sci.*, 2020, **284**, 102267, DOI: **10.1016/j.cis.2020.102267**.

65 R. Xu, F. Gao, Y. Wu, L. Ding, D. Chen, T. Liu, Y. Yu, W. Zhuo, Z. Chen, Y. Zhang, Y. Sun, F. Yang, J. Chen, Y. Cao, J. Kang, Z. Zheng and M. Xiang, Influences of support layer hydrophilicity on morphology and performances of polyamide thin-film composite membrane, *Sep. Purif. Technol.*, 2022, **281**, 119884, DOI: **10.1016/j.seppur.2021.119884**.

66 A. Miao, M. Wei, F. Xu and Y. Wang, Influence of membrane hydrophilicity on water permeability: An experimental study bridging simulations, *J. Membr. Sci.*, 2020, **604**, 118087, DOI: **10.1016/j.memsci.2020.118087**.

67 M. Balouiri, M. Sadiki and S. K. Ibnsouda, Methods for in vitro evaluating antimicrobial activity: A review, *J. Pharm. Anal.*, 2016, **6**, 79, DOI: **10.1016/j.jpha.2015.11.005**.

68 S. Anees Ahmad, S. Sachi Das, A. Khatoon, M. Tahir Ansari, M. Afzal, M. Saquib Hasnain and A. Kumar Nayak, Bactericidal activity of silver nanoparticles: A mechanistic review, *Mater. Sci. Energy Technol.*, 2020, **3**, 769, DOI: **10.1016/j.mset.2020.09.002**.

69 H. S. Vrouwenvelder, J. A. M. Van Paassen, H. C. Folmer, J. A. M. H. Hofman, M. M. Nederlof and D. Van Der Kooij, Biofouling of membranes for drinking water production, *Desalination*, 1998, **118**, 157–166, DOI: **10.1016/S0011-9164(98)00116-7**.

70 X. J. Zha, X. Zhao, J. H. Pu, L. S. Tang, K. Ke, R. Y. Bao, L. Bai, Z. Y. Liu, M. B. Yang and W. Yang, Flexible Anti-Biofouling MXene/Cellulose Fibrous Membrane for Sustainable Solar-Driven Water Purification, *ACS Appl. Mater. Interfaces*, 2019, **11**, 36597, DOI: **10.1021/acsami.9b10606**.

71 Y. Xie, S. Chen, X. Zhang, Z. Shi, Z. Wei, J. Bao, W. Zhao and C. Zhao, Engineering of Tannic Acid Inspired Antifouling and Antibacterial Membranes through Co-deposition of Zwitterionic Polymers and Ag Nanoparticles, *Ind. Eng. Chem. Res.*, 2019, **58**, 11697, DOI: **10.1021/acs.iecr.9b00224**.

72 W. Ha, J. L. Yang and Y. P. Shi, Tannic Acid-Modified Silver Nanoparticles for Antibacterial and Anticancer Applications, *ACS Appl. Nano Mater.*, 2023, **6**, 9627, DOI: **10.1021/acsanm.3c01291**.

73 L. Vásquez, A. Davis, F. Gatto, M. Ngoc An, F. Drago, P. P. Pompa, A. Athanassiou and D. Fragouli, Multifunctional PDMS polyHIPE filters for oil-water separation and antibacterial activity, *Sep. Purif. Technol.*, 2021, **255**, 117748, DOI: **10.1016/j.seppur.2020.117748**.

74 Y. Yao, X. Dang, X. Qiao, R. Li, J. Chen, Z. Huang and Y. K. Gong, Crosslinked biomimetic coating modified stainless-steel-mesh enables completely self-cleaning separation of crude oil/water mixtures, *Water Res.*, 2022, **224**, 119052, DOI: **10.1016/j.watres.2022.119052**.

75 R. Dewi, N. Shamsuddin, M. S. Abu Bakar, S. Thongratkaew, K. Faungnawakij and M. R. Bilad, Development of Tannic Acid Coated Polyvinylidene Fluoride Membrane for Filtration of River Water Containing High Natural Organic Matter, *Science*, 2023, **5**, 42, DOI: **10.3390/sci5040042**.

76 X. Yang, L. Yan, Y. Wu, Y. Liu and L. Shao, Biomimetic hydrophilization engineering on membrane surface for highly-efficient water purification, *J. Membr. Sci.*, 2019, **589**, 117223, DOI: **10.1016/j.memsci.2019.117223**.

77 G. Sathishkumar, K. Gopinath, K. Zhang, E. T. Kang, L. Xu and Y. Yu, Recent progress in tannic acid-driven antibacterial/antifouling surface coating strategies, *J. Mater. Chem. B*, 2022, **10**, 2315, DOI: **10.1039/d1tb02073k**.

78 T. Xiao, Z. Zhu, L. Li, J. Shi, Z. Li and X. Zuo, Membrane fouling and cleaning strategies in microfiltration/ultrafiltration and dynamic membrane, *Sep. Purif. Technol.*, 2023, **318**, 123977, DOI: **10.1016/j.seppur.2023.123977**.

79 M. F. Rabuni, N. M. Nik Sulaiman, M. K. Aroua and N. A. Hashim, Effects of Alkaline Environments at Mild Conditions on the Stability of PVDF Membrane: An Experimental Study, *Ind. Eng. Chem. Res.*, 2013, **52**, 15874–15882, DOI: **10.1021/ie402684b**.

80 M. Li, L. Wu, C. Zhang, W. Chen and C. Liu, Hydrophilic and antifouling modification of PVDF membranes by one-step assembly of tannic acid and polyvinylpyrrolidone, *Appl. Surf. Sci.*, 2019, **483**, 967–978, DOI: **10.1016/j.apsusc.2019.04.057**.

81 X. Ou, X. Yang, J. Zheng and M. Liu, Novel Halloysite Nanotubes Intercalated Graphene Oxide Based Composite Membranes for Multifunctional Applications: Oil/Water Separation and Dyes Removal, *ACS Sustainable Chem. Eng.*, 2019, **7**, 13379–13390, DOI: **10.1021/acs.iecr.7b02723**.

82 W. Zhou, Y. Fang, P. Li, L. Yan, X. Fan, Z. Wang, W. Zhang and H. Liu, Ampholytic Chitosan/Alginate Composite Nanofibrous Membranes with Super Anti-Crude Oil-Fouling Behavior and Multifunctional Oil/Water Separation Properties, *ACS Sustainable Chem. Eng.*, 2019, **7**, 15463–15470, DOI: **10.1021/acssuschemeng.9b03002**.

83 J. M. Luque-Alled, A. Abdel-Karim, M. Alberto, S. Leaper, M. Perez-Page, K. Huang, A. Vijayaraghavan, A. S. El-Kalliny, S. M. Holmes and P. Gorgojo, Polyethersulfone membranes: From ultrafiltration to nanofiltration via the incorporation of APTS functionalized-graphene oxide, *Sep. Purif. Technol.*, 2020, **230**, 115836, DOI: **10.1016/j.seppur.2019.115836**.

84 C. Yang, M. Long, C. Ding, R. Zhang, S. Zhang, J. Yuan, K. Zhi, Z. Yin, Y. Zheng, Y. Liu, H. Wu and Z. Jiang, Antifouling graphene oxide membranes for oil-water separation via hydrophobic chain engineering, *Nat. Commun.*, 2022, **13**, 7334, DOI: **10.1038/s41467-022-35105-8**.

85 O. Srichaiyapol, S. Thammawithan, P. Siritongsuk, S. Nasompag, S. Daduang, S. Klaynongsruang, S. Kulchat and R. Patramanon, Tannic Acid-Stabilized Silver Nanoparticles Used in Biomedical Application as an Effective Antimelioidosis and Prolonged Efflux Pump Inhibitor against Melioidosis Causative Pathogen, *Molecules*, 2021, **26**, 1004, DOI: **10.3390/molecules26041004**.

86 Y. Wang, D. Li, J. Li, J. Li, M. Fan, M. Han, Z. Liu, Z. Li and F. Kong, Metal organic framework UiO-66 incorporated ultrafiltration membranes for simultaneous natural organic matter and heavy metal ions removal, *Environ. Res.*, 2022, **208**, 112651, DOI: **10.1016/j.envres.2021.112651**.

87 L. Fekete, Á. F. Fazekas, C. Hodúr, Z. László, Á. Ágoston, L. Janovák, T. Gyulavári, Z. Pap, K. Hernadi and G. Veréb, Outstanding Separation Performance of Oil-in-Water Emulsions with TiO2/CNT Nanocomposite-Modified PVDF, *Membranes*, 2023, **13**, 209, DOI: **10.3390/membranes13020209**.

88 B. Bolto, J. Zhang, X. Wu and Z. Xie, A Review on Current Development of Membranes for Oil Removal from Wastewaters, *Membranes*, 2020, **10**, 65, DOI: **10.3390/membranes10040065**.

89 M. Gurusamy, S. Thangavel, J. Čespiva, J. Ryšavý, W. M. Yan, M. Jadlovec and G. Arthanareeswaran, An Assessment of the Catalytic and Adsorptive Performances of Cellulose Acetate-Based Composite Membranes for Oil/Water Emulsion Separation, *Polymers*, 2024, **16**, 3108, DOI: **10.3390/polym16223108**.

90 C. Deborah Mbakaogu, N. Claribelle Nwogu, N. Chinedu Izuwa and S. Toochukwu Ekwueme, *Int. J. Oil, Gas Coal Eng.*, 2020, **8**, 151–156, DOI: **10.11648/j.ogce.20200806.15**.

91 D. Mohanadas, P. M. I. Nordin, R. Rohani, N. S. F. Dzulkharnien, A. W. Mohammad, P. Mohamed Abdul and S. Abu Bakar, A Comparison between Various Polymeric Membranes for Oily Wastewater Treatment via Membrane Distillation Process, *Membranes*, 2023, **13**, 46, DOI: **10.3390/membranes13010046**.

92 M. Chen, S. G. J. Heijman, M. W. J. Luiten-Olieman and L. C. Rietveld, Oil-in-water emulsion separation: Fouling of alumina membranes with and without a silicon carbide deposition in constant flux filtration mode, *Water Res.*, 2022, **216**, 118267, DOI: **10.1016/j.watres.2022.118267**.

93 L. T. S. Choong, Y. M. Lin and G. C. Rutledge, Separation of oil-in-water emulsions using electrospun fiber membranes and modeling of the fouling mechanism, *J. Membr. Sci.*, 2015, **486**, 229–238, DOI: **10.1016/j.memsci.2015.03.027**.

94 W. de Melo, G. V. G. Lesak, T. V. de Oliveira, F. A. P. Voll, A. F. Santos and R. B. Vieira, Microfiltration of Oil-in-water Emulsion Using Modified Ceramic Membrane: Surface Properties, Membrane Resistance, Critical Flux, and Cake Behavior, *Mater. Res.*, 2022, **25**, e20210365, DOI: **10.1590/1980-5373-MR-2021-0365**.

95 T. Poyai, P. Khiewpuckdee, A. Wongrueng, P. Painmanakul and N. Chawaloesphonsiya, Enhancement of Crossflow Ultrafiltration for the Treatment of Stabilized Oily Emulsions, *Eng. J.*, 2019, **23**, 15–27, DOI: **10.4186/ej.2019.23.4.15**.

96 R. Goyat, J. Singh, A. Umar, Y. Saharan, A. A. Ibrahim, S. Akbar and S. Baskoutas, Enhancing oil–water emulsion separation via synergistic filtration using graphene oxide–silver oxide nanocomposite-embedded polyethersulfone membrane, *Waste Manage. Res.*, 2024, **42**, 595–607, DOI: **10.1177/0734242X231223914**.

97 E. S. Dmitrieva, T. S. Anokhina, E. G. Novitsky, V. V. Volkov, A. V. Volkov and I. L. Borisov, Polymeric Membranes for Oil-Water Separation: A Review, *Polymers*, 2022, **14**, 980, DOI: **10.3390/polym14050980**.